

## Bimetallic Reactivity. One-Site Addition Two-Metal Oxidation Reaction of Dioxygen with a Bimetallic Dicobalt(II) Complex Bearing Five- and Six-Coordinate Sites

Anna L. Gavrilova,<sup>†</sup> C. Jin Qin,<sup>†</sup> Roger D. Sommer,<sup>‡</sup> Arnold L. Rheingold,<sup>\*,‡</sup> and B. Bosnich<sup>\*,†</sup>

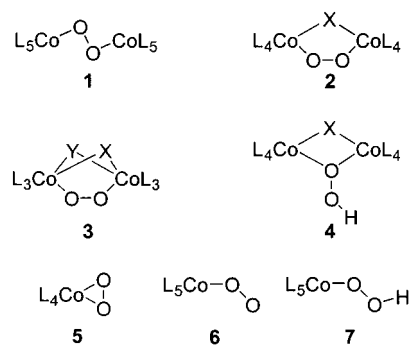
Contribution from the Department of Chemistry, The University of Chicago, 5735 South Ellis Avenue, Chicago, Illinois 60637, and Department of Chemistry and Biochemistry, University of Delaware, Newark, Delaware 19716

Received October 18, 2001

**Abstract:** The di-Co<sup>2+</sup> complex, [Co<sup>2+</sup>(μ-OH)(oxapyme)Co<sup>2+</sup>(H<sub>2</sub>O)]<sup>+</sup>, contains an unsymmetrical binucleating ligand (oxapyme) which provides five- and six-coordinate metal sites when a hydroxide bridge is introduced. This complex absorbs 1 equiv of O<sub>2</sub> irreversibly in solution, producing an unstable di-Co<sup>3+</sup> oxygenated product. The oxygenated product has been studied at low temperatures, where its electronic absorption and <sup>1</sup>H NMR spectra were recorded. It is probable that the oxygenation reaction involves a one-site addition two-metal oxidation reaction to produce an end-on-bonded peroxide ligand at the available coordination site, giving the complex [Co<sup>3+</sup>(μ-OH)(oxapyme)Co<sup>3+</sup>(η<sup>1</sup>-O<sub>2</sub>)]<sup>+</sup>. Addition of 1 equiv of HClO<sub>4</sub> to this oxygenation product gives a stable peroxide complex, [Co<sup>3+</sup>(μ,η<sup>1</sup>:η<sup>2</sup>-O<sub>2</sub>)(oxapyme)Co<sup>3+</sup>]<sup>2+</sup>, where one of the oxygen atoms bridges the two metals and is sideways bonded to one of the metals. The formation of this stable complex involves expulsion of the OH<sup>-</sup> bridge. Addition of NO<sub>2</sub><sup>-</sup> to the sideways-bonded peroxide complex leads to the formation of another stable complex, [Co<sup>3+</sup>(μ,η<sup>1</sup>:η<sup>1</sup>-O<sub>2</sub>)(oxapyme)Co<sup>3+</sup>(NO<sub>2</sub>)]<sup>+</sup>, where the peroxide forms a classic di-end-on bridge to the two metals. Both of these complexes have been fully characterized. Addition of acid to this second stable dioxygen complex leads to the release of HNO<sub>2</sub> and the formation of the μ,η<sup>1</sup>:η<sup>2</sup> sideways-bonded peroxide complex.

### Introduction

The history of dioxygen complexes of Co<sup>3+</sup> extends to the early development of coordination chemistry which employed atmospheric oxygen for the oxidation of Co<sup>2+</sup> complexes to form stable Co<sup>3+</sup> compounds.<sup>1</sup> Even at this stage, a number of intermediate dioxygen complexes were isolated, and their possible structures were inferred. It is now known that dioxygen in compounds of Co<sup>3+</sup> can exist as peroxide or superoxide ligands which can bridge two metals or can be bound to a single metal.<sup>2</sup> The presently known modes of dioxygen binding to octahedral Co<sup>3+</sup> complexes are illustrated in 1–7 (L = ligand; Y, X = one-atom bridging ligand). The most commonly observed dioxygen complexes of Co<sup>3+</sup> are those of the types 1<sup>3</sup> and 2,<sup>4,5</sup> which can exist as complexes supporting peroxide or superoxide ligands; the latter are usually formed by oxidation



of the former that are formed directly from O<sub>2</sub>. The structural type 3, a superoxide complex first prepared by Werner,<sup>1d</sup> has recently been structurally determined.<sup>6</sup> Another Werner-prepared complex,<sup>1d</sup> type 4, an unusual structural type, has also been structurally characterized.<sup>5</sup> The sideways-bonded dioxygen complexes, type 5, prevalent among the early transition elements, are formed with Co<sup>3+</sup> when soft ligands such as tertiary

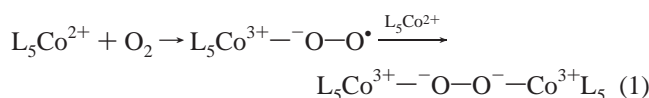
<sup>†</sup> The University of Chicago.

<sup>‡</sup> University of Delaware.

- (1) (a) Frémy, E. *Ann. Chem. Pharm.* **1852**, 83, 227. (b) Frémy, E. *Ann. Chim. Phys.* **1852**, 35, 257. (c) Vortmann, G. *Monatsh. Chem.* **1885**, 6, 404. (d) Werner, A. *Liebigs Ann.* **1910**, 375, 1. (e) Werner, A.; Mylius, A. *Z. Anorg. Chem.* **1898**, 16, 245.  
 (2) Lever, A. B. P.; Gray, H. B. *Acc. Chem. Res.* **1978**, 11, 8.  
 (3) (a) Schmidt, S.; Heinemann, F. W.; Grohmann, A. *Eur. J. Inorg. Chem.* **2000**, 1657. (b) Gatehouse, B. M.; McLachlan, G.; Martin, L. L.; Martin, R. L.; Spiccia, L. *Aust. J. Chem.* **1991**, 44, 351. (c) Curtis, N. F.; Robinson, W. T.; Weatherburn, D. C. *Aust. J. Chem.* **1992**, 45, 1663. (d) Bernhardt, P. V.; Lawrence, G. A.; Hambley, T. W. *J. Chem. Soc., Dalton Trans.* **1990**, 235. (e) Gubelmann, M. H.; Rüttimann, S.; Bocquet, B.; Williams, A. F. *Helv. Chim. Acta* **1990**, 73, 1219.

- (4) (a) Sugimoto, H.; Toshihiko, N.; Maruyama, S.; Fujinami, S.; Yasuda, Y.; Suzuki, M.; Uehara, A. *Bull. Chem. Soc. Jpn.* **1998**, 71, 2267. (b) Kayatani, T.; Hayashi, Y.; Suzuki, M.; Uehara, A. *Bull. Chem. Soc. Jpn.* **1994**, 67, 1980. (c) Suzuki, M.; Sugisawa, T.; Uehara, A. *Bull. Chem. Soc. Jpn.* **1990**, 63, 1115.  
 (5) Thewalt, U.; Marsh, R. *J. Am. Chem. Soc.* **1967**, 89, 6364.  
 (6) Spingler, B.; Scanavy-Grigorieff, M.; Werner, A.; Berke, H.; Lippard, S. *J. Inorg. Chem.* **2001**, 40, 1065.

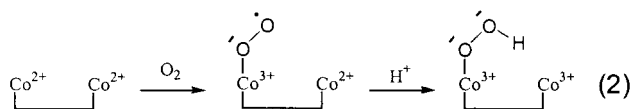
arsines or phosphines are present.<sup>7-9</sup> In contrast, types **1-4** are observed with hard ligands, usually amines and carboxylates. As yet, hard ligands have not provided structurally characterized complexes of type **5**.<sup>7</sup> The dioxygen bonding mode, type **6**, has been characterized in Co<sup>3+</sup> complexes of Schiff bases and porphyrins<sup>10</sup> and with cyanide ligands.<sup>11</sup> All are superoxide complexes. In some of these cases the binding of dioxygen is reversible,<sup>10</sup> as is the case for some of the peroxide complexes of type **2**<sup>4</sup> when binucleating ligands are used. The formation of the superoxide type **6** complexes appears to depend on the ancillary ligands, on the solvent in which the oxygenation occurs, and, in some cases, on temperature. In the absence of steric impediments, type **6** compounds can be regarded as intermediates in the formation of peroxide complexes of type **1**, the formation of which occurs by the steps shown in eq 1, where the type **6** superoxide intermediate couples with L<sub>5</sub>Co<sup>2+</sup> to give the type **1** peroxide product (eq 1). It is probable that



an analogous, but intramolecular, process occurs when binucleating ligands are used for the formation of type **2** complexes.

End-on hydroperoxide complexes of Co<sup>3+</sup>, type **7**, have proved to be the most elusive. Whereas type **7** Co<sup>3+</sup> hydroperoxide complexes are generally expected to be stable, their formation requires two-electron reduction of O<sub>2</sub>, which is not possible using a single Co<sup>2+</sup> complex. A number of possibilities present themselves. One is the use of Co<sup>+</sup> complexes which could provide for the two-electron reduction of O<sub>2</sub>. We are unaware of any reports of such a reaction which gives the type **7** hydroperoxide product. Another method would involve the use of a Co<sup>2+</sup> complex which first would form a type **6** superoxide intermediate which then would be reduced further by an external reductant. This method has recently been employed in the formation of a fully characterized type **7** complex bearing a macrocyclic tetraamine ligand.<sup>12</sup>

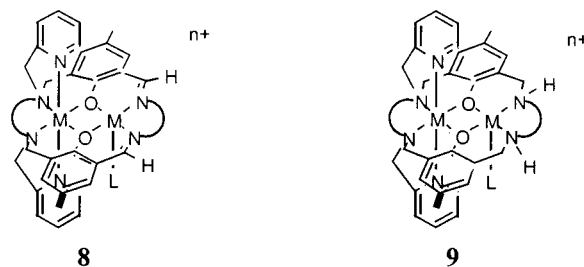
A more direct method of accessing type **7** complexes would involve the synthesis of bimetallic di-Co<sup>2+</sup> complexes which bear five- and six-coordinate sites. With such complexes it is possible to entertain the prospect of O<sub>2</sub> binding to the Co<sup>2+</sup> in the five-coordinate site but being reduced by two electrons, one each for the two Co<sup>2+</sup> ions (eq 2). Such a process requires that



the intramolecular electron transfer in the mixed-valence intermediate be faster than the intermolecular dimerization depicted in eq 1. The sequence outlined in eq 2 can be described

as a one-site addition two-metal oxidation reaction, a process which has only recently been demonstrated in a synthetic cobalt system.<sup>13</sup>

Our initial attempts at achieving one-site addition two-metal oxidation reactions with O<sub>2</sub> and other substrates involved the investigation of the bimetallic complexes of the types **8** and **9**.<sup>14</sup> The Co<sup>2+</sup> ions are in five- and six-coordinate sites, as



required. The loops joining the nitrogen atoms can represent combinations of two or three methylene groups. It was shown that monometallic cobalt complexes of the six-coordinate site readily support the Co<sup>3+</sup> state, and the salen-like five-coordinate site is known to absorb O<sub>2</sub> to give superoxide complexes.<sup>10</sup> Thus, if the reactivity of the bimetallic complexes, **8**, resembles the sum of their parts, they would be expected to absorb O<sub>2</sub> to give the desired di-Co<sup>3+</sup> peroxide (type **7**) complexes. All of the di-Co<sup>2+</sup> complexes, **8**, irrespective of chelate ring size, were found to be inert to O<sub>2</sub>. Neither the addition of ferrocenium ions nor even Br<sub>2</sub> resulted in the formation of di-Co<sup>3+</sup> species. The complexes of **9** were somewhat more reactive. Addition of 1 equiv or more of ferrocenium ions led to the formation of the mixed-valence Co<sup>3+</sup>-Co<sup>2+</sup> complex, where the Co<sup>3+</sup> was in the six-coordinate site. Exposure of the complexes, **9**, to O<sub>2</sub> led to the formation of the other mixed-valence Co<sup>2+</sup>-Co<sup>3+</sup> complexes, where the Co<sup>3+</sup> is now in the other site. When ferrocenium ions were added to these mixed-valence complexes, the Co<sup>2+</sup> in the six-coordinate site was not oxidized to Co<sup>3+</sup>. This mutual oxidative deactivation behavior was observed for other metals and was found to amount to an 18 kcal mol<sup>-1</sup> difference in redox potential between the corresponding monometallic and bimetallic complexes.<sup>14</sup>

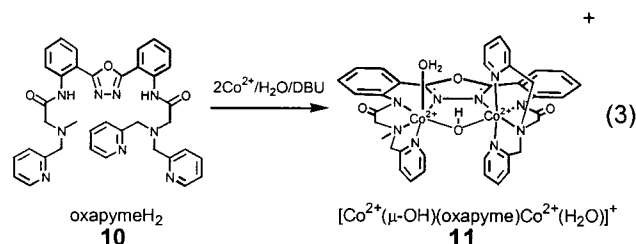
A number of factors were assumed to contribute to the observed mutual deactivation for **9** and the oxidative inertness of **8**.<sup>14</sup> It is believed that the predominant source of the observed oxidative deactivation is mechanical coupling, a conformational effect which couples each metal site. In the case of **8**, the two metal ions are held in a fixed conformation of the ligand, and the bond length and angle changes that accompany metal oxidation are restrained from occurring by the rigid conformation of the ligand. In the case of the more flexible system, **9**, oxidation of one metal leads to conformational changes which are transmitted to the other site and deactivate the other metal

- (7) Bosnich, B.; Boucher, H.; Marshall, C. *Inorg. Chem.* **1976**, *15*, 634.  
 (8) Vaska, L. *Acc. Chem. Res.* **1976**, *9*, 75.  
 (9) Halpern, J.; Goodall, B. L.; Khare, G. P.; Lim, H. S.; Pluth, J. J. *J. Am. Chem. Soc.* **1975**, *97*, 2301.  
 (10) (a) Basolo, F.; Hoffman, B. M.; Ibers, J. A. *Acc. Chem. Res.* **1975**, *8*, 384. (b) McLendon, G.; Martell, A. E. *Coord. Chem. Rev.* **1976**, *19*, 1. (c) Schaefer, W. P.; Huie, B. T.; Kurilla, M. G.; Ealick, S. E. *Inorg. Chem.* **1980**, *19*, 340.  
 (11) (a) White, D. A.; Solodar, A. J.; Baizer, M. M. *Inorg. Chem.* **1972**, *11*, 2160. (b) Brown, L. D.; Raymond, K. N. *Inorg. Chem.* **1975**, *14*, 2595.  
 (12) Guzei, I. A.; Bakac, A. *Inorg. Chem.* **2001**, *40*, 2390.

- (13) Incarvito, C.; Rheingold, A. L.; Gavrilo, A. L.; Qin, C. J.; Bosnich, B. *Inorg. Chem.* **2001**, *40*, 4101.  
 (14) (a) Fraser, C.; Johnston, L.; Rheingold, A. L.; Haggerty, B. S.; Williams, C. K.; Whelan, J.; Bosnich, B. *Inorg. Chem.* **1992**, *31*, 1835. (b) Fraser, C.; Ostrander, R.; Rheingold, A. L.; White, C.; Bosnich, B. *Inorg. Chem.* **1994**, *33*, 324. (c) Fraser, C.; Bosnich, B. *Inorg. Chem.* **1994**, *33*, 338. (d) McCollum, D. G.; Hall, L.; White, C.; Ostrander, R.; Rheingold, A. L.; Whelan, J.; Bosnich, B. *Inorg. Chem.* **1994**, *33*, 924. (e) McCollum, D. G.; Fraser, C.; Ostrander, R.; Rheingold, A. L.; Bosnich, B. *Inorg. Chem.* **1994**, *33*, 2383. (f) McCollum, D. G.; Yap, G. P. A.; Rheingold, A. L.; Bosnich, B. *J. Am. Chem. Soc.* **1996**, *118*, 1365. (g) McCollum, D. G.; Yap, G. P. A.; Liable-Sands, L.; Rheingold, A. L.; Bosnich, B. *Inorg. Chem.* **1997**, *36*, 2230. (h) Bosnich, B. *Inorg. Chem.* **1999**, *38*, 2554.

to oxidation. If this hypothesis is correct, a necessary (but not sufficient) condition for one-site addition two-metal oxidation to occur is the elimination or minimization of mechanical coupling in bimetallic complexes.

For multidentate binucleating ligands, the elimination of mechanical coupling in their bimetallic complexes requires careful consideration of design. We recently reported<sup>13</sup> the preparation of the binucleating ligand, **10**, which forms complexes of the kind **11** with divalent metal ions (eq 3). When a



single exogenous bridge, such as  $\text{OH}^-$ , is incorporated, the unsymmetrical ligand, **10**, generates complexes bearing five- and six-coordinate sites, **11**. Molecular models indicate that complexes form with little strain. They also suggest that the rigid oxadiazole bridging ligand and exogenous  $\text{OH}^-$  bridge will allow conformational changes, which accompany metal oxidation, to be localized to the site of oxidation. That is, two sites should be essentially uncoupled. For  $\text{O}_2$  uptake, the  $\text{OH}^-$  ligand should provide a proton to transfer to the formed end-on peroxide ligand for stability.

Sequential addition of ferrocenium to this di- $\text{Co}^{2+}$  complex leads first to the formation of a mixed-valence  $\text{Co}^{3+}\text{--Co}^{2+}$  complex which, after 2 equiv are added, forms the di- $\text{Co}^{3+}$  complex. This behavior is in sharp contrast to that found for **8** and **9** and suggests that minimal mechanical coupling obtains in the complexes **11**. Following from these results, it was found that the addition of  $\text{NO}_2^+$  and  $\text{Br}_2$  to solutions of the di- $\text{Co}^{2+}$  complexes gave the di- $\text{Co}^{3+}$  nitro and bromo complexes, respectively. Thus, the di- $\text{Co}^{2+}$  complexes, **11**, appear to display the oxidative characteristics which are necessary to obtain one-site addition two-metal oxidation reactions with  $\text{O}_2$ . The di- $\text{Co}^{2+}$  complexes of **11** were found to be  $\text{O}_2$  sensitive both in solution and in the solid state. We report here on the isolation and characterization of a number of these dioxygen cobalt complexes.

## Results

**Dioxygen Reactions.** Exposure of  $[\text{Co}^{2+}(\mu\text{-OH})(\text{oxapyme})\text{Co}^{2+}(\text{H}_2\text{O})]^+$  to  $\text{O}_2$  in dry acetonitrile, acetone, or dimethylformamide solutions at room temperature leads to very rapid formation of deep red-brown solutions which, after a few minutes, fade to a yellow-brown color. The stoichiometry of the  $\text{O}_2$  reaction was determined by volumetric methods, and it was found that 1 molecular equivalent of  $\text{O}_2$  was consumed by 1 equiv of  $[\text{Co}^{2+}(\mu\text{-OH})(\text{oxapyme})\text{Co}^{2+}(\text{H}_2\text{O})]^+$ . The dioxygen reaction was accompanied by the disappearance of a (d-d) electronic absorption band at 1015 nm which is present in the di- $\text{Co}^{2+}$  precursor but is absent in all di- $\text{Co}^{3+}$  complexes.<sup>13</sup>

When the reactions with  $\text{O}_2$  are carried at  $-40^\circ\text{C}$  or lower temperatures in acetonitrile, acetone, and dimethylformamide, the deep red-brown solutions are stable for several hours. The visible absorption spectrum at  $-40^\circ\text{C}$  in acetonitrile solution

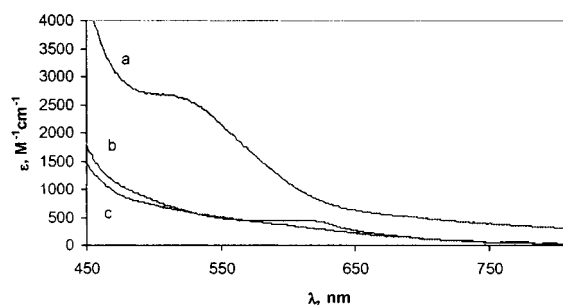


**Figure 1.** Electronic spectra of  $[\text{Co}^{3+}(\mu\text{-OH})(\text{oxapyme})\text{Co}^{3+}(\eta^1\text{-O}_2)]^+$  (a), decomposed  $[\text{Co}^{3+}(\mu\text{-OH})(\text{oxapyme})\text{Co}^{3+}(\eta^1\text{-O}_2)]^+$  (b), and  $[\text{Co}(\mu\text{-OH})(\text{oxapyme})\text{Co}(\text{H}_2\text{O})]^{3+}$  (c) in  $\text{CH}_3\text{CN}$ .

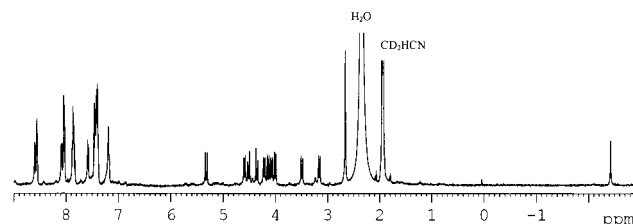
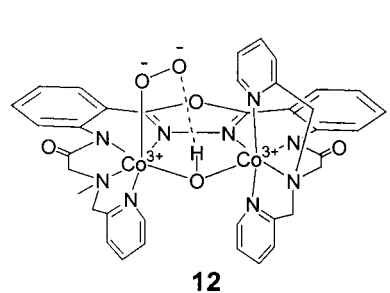


**Figure 2.**  $^1\text{H}$  NMR spectrum of the oxygenation product  $[\text{Co}^{3+}(\mu\text{-OH})(\text{oxapyme})\text{Co}^{3+}(\eta^1\text{-O}_2)]^+$  (**12**) in  $\text{CD}_3\text{CN}$  at  $-40^\circ\text{C}$ .

is shown in Figure 1. The reaction of  $\text{O}_2$  with  $[\text{Co}^{2+}(\mu\text{-OH})(\text{oxapyme})\text{Co}^{2+}(\text{H}_2\text{O})]\text{ClO}_4$  in  $\text{CD}_3\text{CN}$  solutions at  $-40^\circ\text{C}$  results in a sharp  $^1\text{H}$  NMR spectrum (Figure 2), which indicates that the oxygenation product is formed in greater than 90% yield. This  $^1\text{H}$  NMR spectrum is similar to spectra observed for other (diamagnetic) di- $\text{Co}^{3+}$  complexes of this ligand.<sup>13</sup> In particular, complexes of this type,  $[\text{Co}^{3+}(\mu\text{-OH})(\text{oxapyme})\text{Co}^{3+}(\text{X})]^{2+}$  ( $\text{X} = \text{Br}, \text{N}_3^-, \text{NO}_2^-$ ), display a sharp  $^1\text{H}$  NMR OH proton signal in the range  $-2.01$  to  $0.57$  ppm in  $\text{CD}_3\text{CN}$  solutions. The product of oxygenation also displays a sharp  $^1\text{H}$  NMR signal in this region, at  $-2.42$  ppm (Figure 2). Addition of one drop of  $\text{D}_2\text{O}$  to these solutions results in decay of this signal at  $-2.42$  ppm, indicating H/D exchange. Solid samples of the oxygenation product were obtained by low-pressure evaporation of the acetonitrile solution at low temperatures. The solid was found to be  $\sim 80\%$  pure by  $^1\text{H}$  NMR spectroscopy observed at  $-40^\circ\text{C}$  in  $\text{CD}_3\text{CN}$  solution. Both  $^{16}\text{O}_2$  and  $^{18}\text{O}_2$  oxygenation products were isolated as  $\sim 80\%$  pure solids. The above observations suggest that the first-formed oxygenation product is the end-on peroxide complex  $[\text{Co}^{3+}(\mu\text{-OH})(\text{oxapyme})\text{Co}^{3+}(\eta^1\text{-O}_2)]^+$ , **12**.



The hydroperoxide  $^1\text{H}$  NMR proton signals have been observed for a  $\text{Pt}^{4+}$  complex<sup>15</sup> and two  $\text{Rh}^{3+}$  complexes<sup>16,17</sup> and

(15) Wick, D. D.; Goldberg, K. I. *J. Am. Chem. Soc.* **1999**, *121*, 11900.

(16) Suzuki, H.; Matsuura, S.; Moro-oka, Y.; Ikawa, T. *J. Organomet. Chem.* **1985**, *286*, 247.

are found to occur at  $\delta$  6.01,  $\delta$  6.43, and  $\delta$  4.55 ppm, respectively. Although a variety of solvents were used to measure these signals, their chemical shifts are substantially different from that observed for the exchangeable proton of the oxygenation product discussed here. Because the chemical shift of this proton occurs in the same region as that of the OH proton for other di- $\text{Co}^{3+}$  complexes of this ligand and not in the regions observed for other hydroperoxide complexes, the observed chemical shift may suggest that the proton is associated mainly with the OH bridge. If this is so, the peroxide ligand may form a hydrogen bond to the OH proton (as drawn in **12**) rather than a hydroperoxide ligand forming a hydrogen bond to an oxo bridge. It should be noted, however, that we cannot exclude the possibility that the oxygenation product exists as a hydroperoxide ligand in a hydroxo-bridged system, although no  $^1\text{H}$  NMR evidence for this extra proton was found. In this case, the extra proton would be derived from water in the solutions. The O–H stretching frequency of non-hydrogen-bonded hydroperoxide ligands occurs at  $\sim 3500\text{ cm}^{-1}$  and is observed as a sharp absorption.<sup>15,17</sup> The  $\sim 80\%$  pure isolated solid formed from oxygenation displays IR bands in this region, but the band(s) are very broad, with maxima at around  $3400\text{ cm}^{-1}$ . Similar IR absorptions are also observed for other  $[\text{Co}^{3+}(\mu\text{-OH})(\text{oxapyme})\text{Co}^{3+}(\text{X})]^{2+}$  complexes, however, and it is not possible to draw definitive conclusions about the nature of the O–H bonds in the oxygenated complex. The O–O stretching frequencies of peroxide complexes are expected to occur in the region  $750\text{--}920\text{ cm}^{-1}$ .<sup>18</sup> Solid-state FT-IR spectra of the  $^{16}\text{O}_2$  and  $^{18}\text{O}_2$  oxygenation products, both as their  $\text{ClO}_4^-$  and  $\text{PF}_6^-$  salts, were measured. Neither the  $^{16}\text{O}_2$  nor  $^{18}\text{O}_2$  oxygenation products of either salt showed IR bands which could be assigned to the O–O stretch in this region. The IR spectrum has a pronounced and broad ligand absorption centered at  $763\text{ cm}^{-1}$ , and it is possible that the putative O–O stretch is hidden by this absorption. FT-Raman spectroscopy on both the  $^{16}\text{O}_2$  and  $^{18}\text{O}_2$  oxygenation products as solid  $\text{PF}_6^-$  salts did not produce absorptions in the expected regions, possibly because of laser light decomposition of the (spinning) samples. Electrospray ionization–mass spectrometry (ESI-MS) proved ineffective in detecting the incorporation of dioxygen because, in acetonitrile solutions, decomposition occurred before entry into the plasma chamber.

The decomposition of the oxygenation product is complicated. Oxygenation of  $[\text{Co}^{2+}(\mu\text{-OH})(\text{oxapyme})\text{Co}^{2+}(\text{H}_2\text{O})]^{2+}$  is irreversible, as evidenced by the fact that at  $-40\text{ }^\circ\text{C}$  in acetonitrile solutions, the color of the oxygenated product does not change when the pressure is lowered to 0.5 mm. Consequently, decomposition probably involves the dissociation of the peroxide ligand. Hydrogen peroxide, however, is not detected by  $^1\text{H}$  NMR spectroscopy (in  $\text{CD}_3\text{CN}$ ). The yellow-brown solution that is formed after decomposition has a visible absorption spectrum which is very similar but not identical to the spectrum of  $[\text{Co}^{3+}(\mu\text{-OH})(\text{oxapyme})\text{Co}^{3+}(\text{H}_2\text{O})]^{3+}$  in acetonitrile solution<sup>13</sup> (Figure 1). The  $^1\text{H}$  NMR spectrum of the decomposed solutions is broad, indicating the presence of  $\text{Co}^{2+}$  species. These solutions catalyze the decomposition of  $\text{H}_2\text{O}_2$ . Thus, when (aqueous)  $\text{H}_2\text{O}_2$  is added

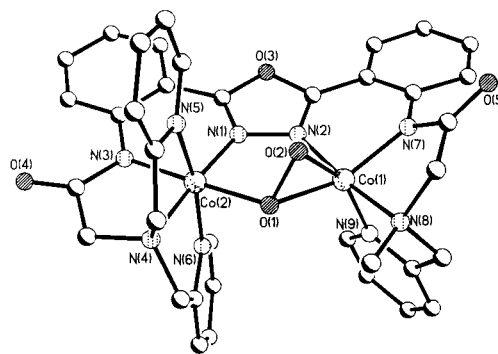


**Figure 3.** Structure of  $[\text{Co}(\mu,\eta^1:\eta^2\text{-O}_2)(\text{oxapyme})\text{Co}](\text{PF}_6)_2\cdot\text{CH}_3\text{CN}$  (**13**). Hydrogen atoms, counterions, and lattice solvent are omitted for clarity.

to these decomposition solutions, vigorous evolution of  $\text{O}_2$  is observed which is accelerated by the addition of a base such as 1,8-diazabicyclo[5.4.0]undec-7-ene (DBU). The decomposition of peroxide is accompanied by an induction period if the decomposition solutions are allowed to stand at  $25\text{ }^\circ\text{C}$  for less than an hour. It appears that the decomposition product develops a small amount of catalytic species. Presumably this is the reason that no  $\text{H}_2\text{O}_2$  is detected by  $^1\text{H}$  NMR spectroscopy in the decomposed solutions. It is perhaps surprising that a  $\text{Co}^{3+}$  complex should be labile, but ligand lability is a characteristic of di- $\text{Co}^{3+}$  complexes of the present ligand.<sup>13</sup> The lability may be due to the presence of a cis-amido ligand which may labilize the peroxide ligand in a manner reminiscent of the  $\text{SN}^1\text{CB}$  mechanism.<sup>19</sup>

**Stable Dioxxygen Complex, 13.** If the oxygenated complex, prepared at  $-40\text{ }^\circ\text{C}$  in acetonitrile solution, is treated with 1 equiv of (aqueous)  $\text{HClO}_4$ , the solution immediately becomes yellow. After the solution is allowed to warm to room temperature, an orange solution is formed, and after the solvent is removed by evaporation, the residue consists of two products, a compound with the formula  $[\text{Co}(\text{O}_2)(\text{oxapyme})\text{Co}]^{2+}$  (80%) and the previously prepared compound,<sup>13</sup>  $[\text{Co}(\mu\text{-OH})(\text{oxapyme})\text{Co}(\text{H}_2\text{O})]^{3+}$  (20%). Dilute solutions (see Experimental Section) are required to obtain a good yield of the first complex, and it was found that this compound could be prepared on a larger scale by the following method in methanol solution. The  $[\text{Co}^{2+}(\mu\text{-OH})(\text{oxapyme})\text{Co}^{2+}(\text{H}_2\text{O})]\text{ClO}_4$  complex was oxygenated at  $-78\text{ }^\circ\text{C}$ , and after the solution was allowed to warm to  $-10\text{ }^\circ\text{C}$ , either  $\text{NH}_4\text{ClO}_4$  or  $\text{NH}_4\text{PF}_6$  was added. After filtration, the red-brown solid was recrystallized from acetonitrile by methanol diffusion. Red-brown crystals formed which displayed a  $^1\text{H}$  NMR spectrum identical to that of the major product from the reaction of  $\text{HClO}_4$  just described. It should be noted that ammonium ions are required to obtain the product in the preparative reaction. The dioxxygen complex is not formed with other (nonprotic)  $\text{ClO}_4^-$  or  $\text{PF}_6^-$  salts.

The solid-state structure of  $[\text{Co}(\text{O}_2)(\text{oxapyme})\text{Co}](\text{PF}_6)_2\cdot\text{CH}_3\text{CN}$ , **13**, is shown in Figure 3, and crystallographic data and a list of selected bond lengths and bond angles are provided in Tables 1 and 2. The dioxxygen binding mode is unusual and appears to be unique for a  $\text{Co}^{3+}$  complex. A dimeric  $\text{Rh}^{3+}$  complex does display this dioxxygen bonding mode, however.<sup>20</sup> The diamagnetism of the complex and the O–O bond length

(17) Carmona, D.; Lamata, M. P.; Ferrer, J.; Modrego, J.; Perales, M.; Lahoz, F. J.; Atencio, R.; Oro, L. A. *J. Chem. Soc., Chem. Commun.* **1994**, 575.

(18) Nakamoto, K. *Infrared and Raman Spectra of Inorganic and Coordination Compounds*, 4th ed.; John Wiley & Sons: New York, 1986; p 311.

(19) Basolo, F.; Pearson, R. G. *Mechanisms of Inorganic Reactions. A Study of Metal Complexes in Solution*, 2nd ed.; John Wiley & Sons: New York, 1973; pp 183–184.

**Table 1.** Crystallographic Data for  $[\text{Co}(\mu, \eta^1: \eta^2\text{-O}_2)(\text{oxapyne})\text{Co}(\text{PF}_6)_2 \cdot \text{CH}_3\text{CN}$  (**13**) and  $[\text{Co}(\mu, \eta^1: \eta^1\text{-O}_2)(\text{oxapyne})\text{Co}(\text{NO}_2)](\text{PF}_6)_2 \cdot 2\text{CH}_3\text{CN}$  (**14**)

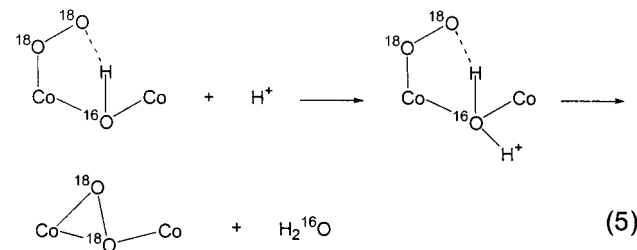
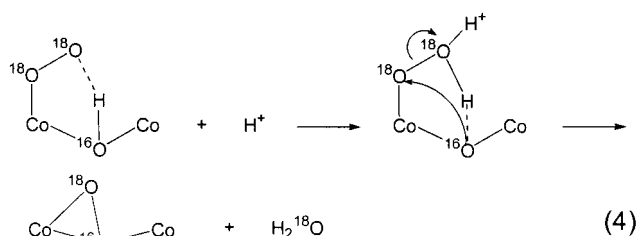
	13	14
formula	$\text{C}_{39}\text{H}_{36}\text{Co}_2\text{F}_{12}\text{N}_{10}\text{O}_5\text{P}_2$	$\text{C}_{41}\text{H}_{39}\text{Co}_2\text{F}_6\text{N}_{12}\text{O}_7\text{P}$
formula weight	1132.58	1074.67
color, crystal habit	red blade	red needle
crystal size, mm	$0.06 \times 0.10 \times 0.10$	$0.04 \times 0.04 \times 0.08$
crystal system	monoclinic	triclinic
space group	$P2_1/n$	$P\bar{1}$
<i>a</i> , Å	12.4805(10)	10.4971(11)
<i>b</i> , Å	18.1277(14)	11.3830(13)
<i>c</i> , Å	18.8005(15)	19.466(2)
$\alpha$ , deg	90	91.013(2)
$\beta$ , deg	91.808(2)	101.484(2)
$\gamma$ , deg	90	110.070(2)
volume, Å <sup>3</sup>	4251.4(6)	2131.6(4)
<i>Z</i>	4	2
<i>T</i> , K	173(2)	173(2)
<i>D</i> (calc), g cm <sup>-3</sup>	1.769	1.674
$\mu$ (Mo K $\alpha$ ), cm <sup>-1</sup>	1.926(4)	9.10
rfins (collected, indep)	21 136, 9205	16 546, 7484
<i>R</i> ( <i>F</i> ), <i>R</i> (w <i>F</i> <sup>2</sup> ), %	7.64, 15.17	5.74, 10.70

$$^a R(F) = \frac{\sum ||F_o| - |F_c||}{\sum |F_o|}; R(wF^2) = \frac{\sum [w(F_o^2 - F_c^2)^2]}{\sum [w(F_o^2)^2]}^{1/2}; w^{-1} = F^2(F_o^2) + (aP)^2 + bP; P = [2F_c^2 + \max(F_o^2, 0)]/3.$$

**Table 2.** Selected Bond Lengths and Angles for  $[\text{Co}(\mu, \eta^1: \eta^2\text{-O}_2)(\text{oxapyne})\text{Co}(\text{PF}_6)_2 \cdot \text{CH}_3\text{CN}$  (**13**)

Bond Lengths (Å)			
Co(1)–O(2)	1.846(4)	Co(2)–N(1)	1.860(5)
Co(1)–N(2)	1.868(6)	Co(2)–O(1)	1.922(5)
Co(1)–N(7)	1.919(5)	Co(2)–N(4)	1.923(5)
Co(1)–O(1)	1.926(4)	Co(2)–N(3)	1.923(6)
Co(1)–N(9)	1.943(6)	Co(2)–N(6)	1.934(5)
Co(1)–N(8)	1.946(6)	Co(2)–N(5)	1.950(5)
O(1)–O(2)	1.456(5)	Co(1)–Co(2)	3.339(5)
Bond Angles (deg)			
O(2)–Co(1)–N(2)	88.3(2)	N(1)–Co(2)–O(1)	88.3(2)
O(2)–Co(1)–N(7)	107.6(2)	N(1)–Co(2)–N(4)	176.2(3)
N(2)–Co(1)–N(7)	89.3(3)	O(1)–Co(2)–N(4)	88.9(2)
O(2)–Co(1)–O(1)	45.33(17)	N(1)–Co(2)–N(3)	91.2(3)
N(2)–Co(1)–O(1)	87.6(2)	O(1)–Co(2)–N(3)	178.5(2)
N(7)–Co(1)–O(1)	152.8(2)	N(4)–Co(2)–N(3)	91.6(3)
O(2)–Co(1)–N(9)	156.9(2)	N(1)–Co(2)–N(6)	94.3(2)
N(2)–Co(1)–N(9)	98.8(2)	O(1)–Co(2)–N(6)	90.3(2)
N(7)–Co(1)–N(9)	94.5(2)	N(4)–Co(2)–N(6)	83.2(2)
O(1)–Co(1)–N(9)	112.7(2)	N(3)–Co(2)–N(6)	91.2(2)
O(2)–Co(1)–N(8)	90.0(2)	N(1)–Co(2)–N(5)	98.2(2)
N(2)–Co(1)–N(8)	173.0(2)	O(1)–Co(2)–N(5)	90.3(2)
N(7)–Co(1)–N(8)	84.8(3)	N(4)–Co(2)–N(5)	84.3(2)
O(1)–Co(1)–N(8)	95.9(2)	N(3)–Co(2)–N(5)	88.4(2)
N(9)–Co(1)–N(8)	85.4(3)	N(6)–Co(2)–N(5)	167.5(2)
O(2)–O(1)–Co(2)	109.1(3)	Co(2)–O(1)–Co(1)	120.4(2)
O(2)–O(1)–Co(1)	64.4(2)	O(1)–O(2)–Co(1)	70.2(2)

(1.456(5) Å) indicate that the dioxygen moiety is best described as a peroxide ligand. The peroxide ligand adopts a “sideways” bonding mode to one  $\text{Co}^{3+}$ , and one of the oxygen atoms bridges to the two metals. The  $\text{Co}^{3+}$  ion bearing the sideways  $\text{O}_2^{2-}$  ligand is in a distorted octahedral geometry; otherwise, the bond lengths and angles are those expected for  $\text{Co}^{3+}$  complexes. As noted earlier, sideways-bonded dioxygen complexes of  $\text{Co}^{3+}$  have only been structurally characterized for compounds bearing soft ligands such as arsines and phosphines.<sup>7–9</sup> The conversion of the first-formed dioxygen complex, **12**, to **13** raises the question of whether the transformation occurs by dioxygen bond scission (eq 4) or by expulsion of the OH bridge (eq 5). As



illustrated in eqs 4 and 5, by using  $^{18}\text{O}_2$  and a  $^{16}\text{OH}$  bridge, dioxygen bond scission leads to an  $^{18}\text{O}-^{16}\text{O}$  peroxo ligand, whereas expulsion of the  $^{16}\text{OH}$  bridge leads to the  $^{18}\text{O}_2$  analogue. The oxygenation reaction was carried out using  $^{18}\text{O}_2$  the di- $\text{Co}^{2+}$  complex with an  $^{16}\text{OH}$  bridge, and the product, **12**, was transformed to **13** by the addition of  $\text{HClO}_4$  in acetonitrile solution. The ESI-MS showed that  $^{18}\text{O}-^{18}\text{O}$  was present in the  $[\text{Co}(\mu, \eta^1: \eta^2\text{-O}_2)(\text{oxapyne})\text{Co}]^{2+}$  product. If  $^{16}\text{O}_2$  is used, ESI-MS spectroscopy gave ions corresponding to the  $^{16}\text{O}-^{16}\text{O}$  complex. These results clearly indicate that the transformation of **12** to **13** involves the removal of the hydroxide bridge (eq 5).

It appears that if the oxygenation is carried out in the methanol solution, as described, the oxygenation product does not contain an OH bridge. If  $\text{NaClO}_4$ , rather than  $\text{NH}_4\text{ClO}_4$ , is added to the methanol oxygenated solution at low temperature, an unstable powder is isolated that has a  $^1\text{H}$  NMR spectrum that shows no OH proton signal. It resembles the spectrum observed for the complex **14** (see later) and carries a signal that can be assigned to a methoxy group. Addition of acid to an acetonitrile solution of this material gives  $[\text{Co}(\mu, \eta^1: \eta^2\text{-O}_2)(\text{oxapyne})\text{Co}]^{2+}$  and methanol. Thus, the necessity of using protic salts, such as  $\text{NH}_4\text{-ClO}_4$ , to isolate the  $[\text{Co}(\mu, \eta^1: \eta^2\text{-O}_2)(\text{oxapyne})\text{Co}]^{2+}$  ion from the preparative reaction in methanol is related to the removal of a methoxy ligand. A similar process is described later (Scheme 1).

FT-Raman spectroscopy was used to obtain the  $^{16}\text{O}-^{16}\text{O}$  and  $^{18}\text{O}-^{18}\text{O}$  stretching frequencies of solid samples of the  $\text{PF}_6^-$  salts of **13**. The  $^{16}\text{O}-^{16}\text{O}$  stretch occurred at  $839\text{ cm}^{-1}$ , and that of  $^{18}\text{O}-^{18}\text{O}$  was observed at  $796\text{ cm}^{-1}$ , a shift of  $43\text{ cm}^{-1}$ , which is less than the  $48\text{ cm}^{-1}$  expected on the basis of the reduced masses. The visible electronic absorption spectrum of **13** is given in Figure 4, and the FT-Raman spectrum is shown in Figure 5.

**Stable Dioxygen Complex, 14.** The sideways binding mode of the peroxide ligand of the complex  $[\text{Co}(\mu, \eta^1: \eta^2\text{-O}_2)(\text{oxapyne})\text{Co}]^{2+}$ , **13**, is expected to engender strain in the associated  $\text{Co}^{3+}$  bonds. Consequently, addition of a unidentate ligand to **13** might be expected to rupture the sideways bonding. This is so, and addition of  $\text{NO}_2^-$  ions to a solution of  $[\text{Co}(\mu, \eta^1: \eta^2\text{-O}_2)(\text{oxapyne})\text{Co}]^{2+}$  leads to the immediate formation of a dark red complex of the formula  $[\text{Co}(\text{O}_2)(\text{oxapyne})\text{Co}(\text{NO}_2)]^+$ , **14**.

(20) (a) Bennett, M. J.; Donaldson, P. B. *Inorg. Chem.* **1977**, *16*, 1585. (b) Sharp, P. R.; Hoard, D. W.; Barnes, C. L. *J. Am. Chem. Soc.* **1990**, *112*, 2024.

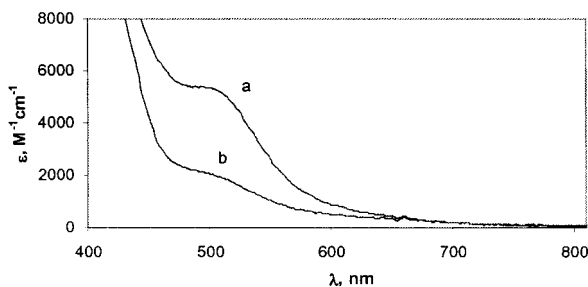


**Figure 4.** Electronic spectra of  $[\text{Co}(\mu,\eta^1:\eta^1\text{-O}_2)(\text{oxapyme})\text{Co}(\text{NO}_2)]^+$  (a) and  $[\text{Co}(\mu,\eta^1:\eta^2\text{-O}_2)(\text{oxapyme})\text{Co}]^{2+}$  (b) in  $\text{CH}_3\text{CN}$ .

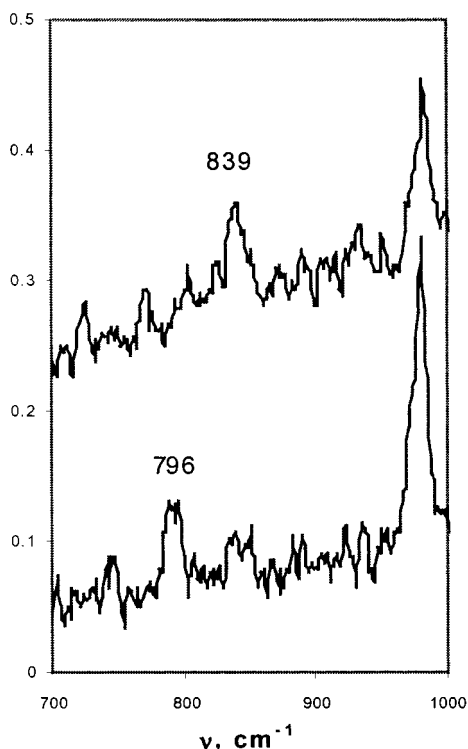
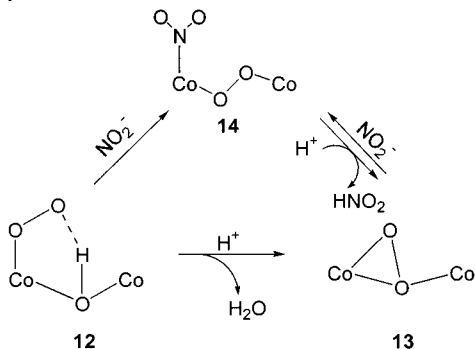


**Figure 5.** FT-Raman spectra of  $^{16}\text{O}_2$ - (top) and  $^{18}\text{O}_2$ -labeled (bottom)  $[\text{Co}(\mu,\eta^1:\eta^2\text{-O}_2)(\text{oxapyme})\text{Co}](\text{PF}_6)_2 \cdot 2\text{CH}_3\text{CN}$  (**13**).

#### Scheme 1



Vapor diffusion of ethanol to an acetone/acetonitrile solution of the  $\text{PF}_6^-$  salt gave crystals of the composition  $[\text{Co}(\text{O}_2)(\text{oxapyme})\text{Co}(\text{NO}_2)](\text{PF}_6)_2 \cdot 2\text{CH}_3\text{CN}$ , **14**. The solid-state structure of this complex is shown in Figure 6. The crystallographic data are provided in Table 1, and selected bond lengths and bond angles are listed in Table 3.

The dioxxygen bonding is in one of the classic bridging modes ( $\mu,\eta^1:\eta^1\text{-O}_2$ ). The O–O bond length (1.409(4) Å) indicates the presence of a bridging peroxide ligand. Consistently, the FT-

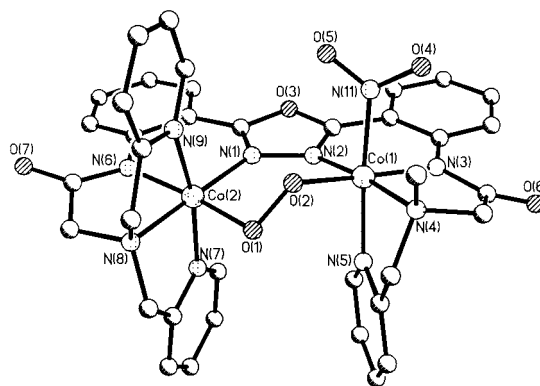


**Figure 6.** Structure of  $[\text{Co}(\mu,\eta^1:\eta^1\text{-O}_2)(\text{oxapyme})\text{Co}(\text{NO}_2)](\text{PF}_6)_2 \cdot 2\text{CH}_3\text{CN}$  (**14**). Hydrogen atoms, counterions, and lattice solvent are omitted for clarity.

**Table 3.** Selected Bond Lengths and Angles for  $[\text{Co}(\mu,\eta^1:\eta^1\text{-O}_2)(\text{oxapyme})\text{Co}(\text{NO}_2)](\text{PF}_6)_2 \cdot 2\text{CH}_3\text{CN}$  (**14**)

Bond Lengths (Å)			
Co(1)–O(2)	1.854(3)	Co(2)–O(1)	1.858(3)
Co(1)–N(2)	1.903(4)	Co(2)–N(1)	1.932(4)
Co(1)–N(11)	1.937(5)	Co(2)–N(8)	1.934(4)
Co(1)–N(3)	1.963(4)	Co(2)–N(9)	1.949(4)
Co(1)–N(4)	1.972(4)	Co(2)–N(7)	1.954(4)
Co(1)–N(5)	1.972(4)	Co(2)–N(6)	2.005(4)
O(1)–O(2)	1.409(4)	Co(1)–Co(2)	3.772(5)
Bond Angles (deg)			
O(2)–Co(1)–N(2)	91.02(16)	O(1)–Co(2)–N(1)	92.73(16)
O(2)–Co(1)–N(11)	89.38(17)	O(1)–Co(2)–N(8)	86.36(17)
N(2)–Co(1)–N(11)	88.71(18)	N(1)–Co(2)–N(8)	178.95(19)
O(2)–Co(1)–N(3)	174.70(15)	O(1)–Co(2)–N(9)	91.29(16)
N(2)–Co(1)–N(3)	93.01(17)	N(1)–Co(2)–N(9)	96.67(17)
N(11)–Co(1)–N(3)	87.27(18)	N(8)–Co(2)–N(9)	83.87(17)
O(2)–Co(1)–N(4)	86.81(16)	O(1)–Co(2)–N(7)	88.23(16)
N(2)–Co(1)–N(4)	174.50(18)	N(1)–Co(2)–N(7)	95.78(17)
N(11)–Co(1)–N(4)	96.31(19)	N(8)–Co(2)–N(7)	83.68(17)
N(3)–Co(1)–N(4)	89.47(17)	N(9)–Co(2)–N(7)	167.55(18)
O(2)–Co(1)–N(5)	95.46(16)	O(1)–Co(2)–N(6)	175.16(16)
N(2)–Co(1)–N(5)	92.42(17)	N(1)–Co(2)–N(6)	91.97(17)
N(11)–Co(1)–N(5)	175.01(19)	N(8)–Co(2)–N(6)	88.94(18)
N(3)–Co(1)–N(5)	87.82(17)	N(9)–Co(2)–N(6)	89.36(17)
N(4)–Co(1)–N(5)	82.77(17)	N(7)–Co(2)–N(6)	90.09(17)
O(1)–O(2)–Co(1)	110.8(2)	O(2)–O(1)–Co(2)	111.1(2)

Raman  $^{16}\text{O}$ – $^{16}\text{O}$  stretching frequency is at  $866\text{ cm}^{-1}$ , and that of  $^{18}\text{O}$ – $^{18}\text{O}$  is at  $825\text{ cm}^{-1}$ , a difference of  $41\text{ cm}^{-1}$  (Figure 7). The metal–ligand bond lengths and angles are unexceptional. The visible absorption spectrum is shown in Figure 4, and the ESI-MS for the  $^{16}\text{O}_2$  and  $^{18}\text{O}_2$  complexes gives parent ions of the correct mass/charge ratios.

**Interconversion of Dioxxygen Complexes.** The complexes **12**, **13**, and **14** undergo a number of unusual transformations. These are summarized in Scheme 1. The reactions **12**  $\rightarrow$  **13** and **13**  $\rightarrow$  **14** have been described. Addition of a methanol solution of  $\text{NaNO}_2$  at  $-40\text{ }^\circ\text{C}$  to an acetonitrile solution of **12** causes the solution to lighten in color, and, after the solution was allowed to warm to room temperature, a bright red solution of **14** is formed in 90% yield. Addition of 1 equiv of  $\text{HPF}_6$  to an acetonitrile solution of **14** causes immediate, quantitative conversion of **14** to **13**. Whether some or all of these interconversions proceed by an intramolecular or an intermolecular mechanism, where, in the latter, dissociation of the peroxide ligand occurs, has not been established. The conversion of **14**  $\rightarrow$  **13** is of particular interest with respect to ligand lability in these  $\text{Co}^{3+}$  complexes and with regard to the stability of the dioxxygen bonding mode in **13**. Addition of  $\text{NH}_3$  or  $\text{Cl}^-$  to **13**

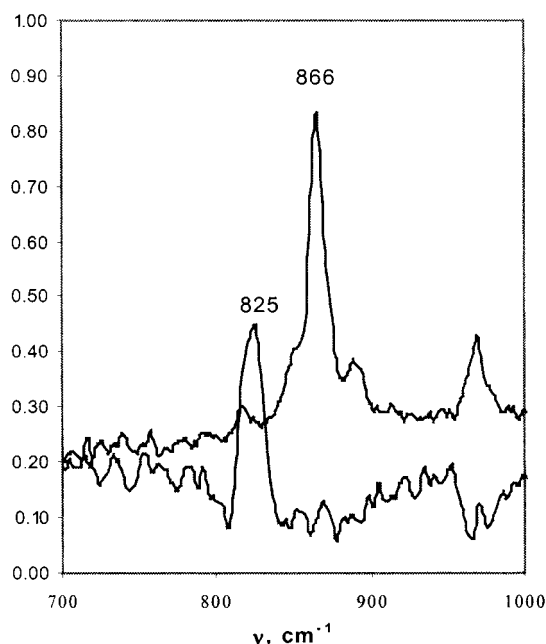


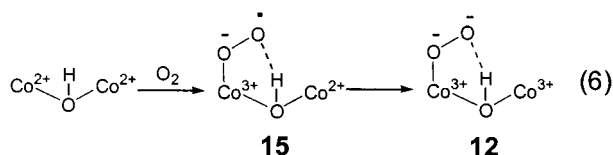
**Figure 7.** FT-Raman spectra of  $^{16}\text{O}_2$ - (top) and  $^{18}\text{O}_2$ -labeled (bottom)  $[\text{Co}(\mu,\eta^1:\eta^1\text{-O}_2)(\text{oxapyme})\text{Co}(\text{NO}_2)](\text{PF}_6)\cdot 2\text{CH}_3\text{CN}$  (**14**).

leads to the formation of complexes analogous to **14**, but the products are in equilibrium with **13**. With  $\text{NO}_2^-$ , the equilibrium is driven completely to **14**. Even so, 1 equiv of acid is sufficient to drive **14** to **13**. It is clear from these results that the sixth ligand in these  $\text{Co}^{3+}$  complexes is labile, and the dioxygen bonding mode in **13** is relatively stable. The sixth ligand lability in these complexes must, at least in part, account for the instability of **12**.

## Discussion

The work described here serves to illustrate two conceptually engaging aspects of bimetallic reactivity. One is related to the phenomenon of one-site addition two-metal oxidation reactions, and the other concerns the interconversion of dioxygen binding modes in bimetallic complexes.

Given that one  $\text{O}_2$  reacts with a molecule of the di- $\text{Co}^{2+}$  complex and essentially pure di- $\text{Co}^{3+}$  product is formed, it is highly probable that this oxygenation reaction is an example of an intramolecular one-site addition two-metal oxidation reaction (eq 6). The process in eq 6 involves, first, the formation of a



mixed-valence superoxide complex, **15**, where the superoxide resides in the five-coordinate site. Transference of an electron from the  $\text{Co}^{2+}$  ion in the six-coordinate site leads to the di- $\text{Co}^{3+}$ -peroxide product, **12**. Whereas there is no doubt that a di- $\text{Co}^{3+}$ -peroxide product is formed, its precise structure could not be established because of its instability. Similarly, the involvement or otherwise of the OH proton in **15** and **12** has not been determined. That an OH proton is present in **12** is secure, however. As noted earlier, the  $^1\text{H}$  NMR chemical shift of this proton occurs at the upfield regions where other di- $\text{Co}^{3+}$

complexes of the present ligand display their OH protons and not in a region where hydroperoxide proton chemical shifts occur. These observations suggest that the OH proton is not transferred to the peroxide ligand, although it might be hydrogen-bonded to it, as shown. If this is the case, proton coupling in the electron-transfer process may be weak. Attempts have been made to ascertain the acidity of the OH proton, but the results were inconclusive. Thus, addition of DBU or Proton Sponge (1,8-bis(dimethylamino)naphthalene) to  $[\text{Co}(\mu\text{-OH})(\text{oxapyme})\text{Co}(\text{X})]^{2+}$  ( $\text{X} = \text{Br}, \text{NO}_2$ ) in acetonitrile solution at  $20^\circ\text{C}$  led to varying degrees of decomposition, depending on the amount of base added, as judged by  $^1\text{H}$  NMR spectroscopy. Although some decomposition occurs, the upfield OH proton signal remained after 1 equiv of base was added, although after several hours the signal disappeared, but at this stage extensive decomposition had occurred. Although inconclusive, these results may indicate, perhaps surprisingly, that the OH proton is not very acidic. Aside from the effects of ligand characteristics, it may be that more oxophilic metals, such as  $\text{Fe}^{3+}$ , are required to obtain proton transfer from the OH to the peroxide. Overall, the oxygenation results, and previous observations,<sup>13</sup> indicate that the binucleating oxapyme ligand does not impose serious mechanical coupling deactivation in one-site addition two-metal oxidation reactions.

The other discovery of this study is the surprisingly facile transformations of the dioxygen ligand in these complexes (Scheme 1). Although bimetallic complexes bearing five- and six-coordinate sites provide a formal method of generating end-on hydroperoxide ligands, they are also prone to the formation of, presumably more stable, bridging peroxide complexes if the bridge(s) are sufficiently labile. It was surprising to find that the OH bridge in the present system could be so readily expelled. In the case of analogous di- $\text{Fe}^{2+}$  complexes, proton transfer from the OH bridge to the dioxygen ligand may be promoted by the stability of the di- $\text{Fe}^{3+}$ -oxo bridge. The stability of the di- $\text{Fe}^{3+}$ -oxo bridge may also restrain the dioxygen ligand from forming dioxygen bridging compounds of the kind described here. It thus appears that, with bimetallic complexes bearing OH bridges, the stability of the end-on hydroperoxide ligand depends to some extent on the OH bridge proton acidity and on the stability of the bridge.

## Experimental Section

**General Procedures and Methods.** All reagents were obtained from commercial suppliers and were used without further purification unless otherwise noted.  $^{18}\text{O}_2$  (99% pure) was purchased from Isotec, Inc., and  $\text{CD}_3\text{CN}$  was purchased from Cambridge Isotope Laboratories, Inc. The  $[\text{Co}(\mu\text{-OH})(\text{oxapyme})\text{Co}(\text{H}_2\text{O})]\text{ClO}_4$  complex was prepared as described previously.<sup>13</sup> All preparations of  $\text{Co}(\text{II})$  complexes were conducted under  $\text{N}_2$  using deaerated solvents and using standard Schlenk techniques. Acetonitrile was dried over  $\text{CaH}_2$ . Ethanol refers to absolute ethanol. FT-infrared spectra were recorded on a Nicolet Nexus 470 FT-IR spectrometer on solid samples. FT-Raman spectra were recorded at  $25^\circ\text{C}$  on crystalline solids in spinning capillary tubes using a Nicolet 950 spectrometer (Nd:YVO<sub>4</sub> source,  $\lambda = 1064\text{ nm}$ , 0.2 mW power) at  $4\text{ cm}^{-1}$  resolution. A total of 1500 scans were collected for each sample. The Raman signal was detected with a liquid-nitrogen-cooled high-purity germanium diode detector (Applied Detector Corp., model 203NR). Raman shifts were calibrated with indene as an external standard. Electronic absorption spectra were obtained with a Perkin-Elmer Lambda 40 UV/VIS spectrophotometer and a Cary 14DS UV/VIS/NIR spectrophotometer. Electronic absorption spectra at  $-40^\circ\text{C}$

were obtained using an HP 8452A diode array spectrophotometer. The wavelength at maximum absorbance ( $\lambda_{\text{max}}$ ) is given in nanometers, and the extinction coefficient ( $\epsilon$ ) in  $\text{M}^{-1} \text{cm}^{-1}$ . Elemental analyses were performed by Desert Analytics Laboratory, Tucson, AZ. Conductance measurements were made at 25 °C in dry acetonitrile or methanol using  $1.0 \times 10^{-3} \text{ M}$  samples and a YSI Scientific model 35 conductance meter.  $^1\text{H}$  NMR spectra were recorded either on Bruker DRX400 or DMX500 Fourier transform spectrometers. Chemical shifts ( $\delta$ ) are given in ppm, and coupling constants ( $J$ ) are given in hertz.

**Measurement of the Visible Absorption Spectrum and  $^1\text{H}$  NMR Spectrum of the Product Formed from the Reaction of Dioxygen with  $[\text{Co}(\mu\text{-OH})(\text{oxapyne})\text{Co}(\text{H}_2\text{O})](\text{ClO}_4)$ .** The  $[\text{Co}(\mu\text{-OH})(\text{oxapyne})\text{Co}(\text{H}_2\text{O})]\text{ClO}_4$  complex (1.6 mg,  $1.8 \mu\text{mol}$ ) was dissolved in dry, deaerated acetonitrile (4 mL) at 25 °C. The yellow solution was cooled to  $-40$  °C, and dioxygen gas was introduced to the stirred solution. The visible absorption spectrum of the resultant dark red solution was measured at this temperature.

The  $^1\text{H}$  NMR spectrum of the oxygenated product at  $-40$  °C in  $\text{CD}_3\text{CN}$  was obtained as follows. The  $[\text{Co}(\mu\text{-OH})(\text{oxapyne})\text{Co}(\text{H}_2\text{O})]\text{ClO}_4$  complex (0.9 mg,  $1 \mu\text{mol}$ ) was dissolved in  $\text{CD}_3\text{CN}$  (99.98% D) ( $0.5 \text{ mL}$ ) at 25 °C in an NMR tube. The yellow solution was cooled to  $-40$  °C, and dioxygen was introduced to give a dark red solution. The  $^1\text{H}$  NMR spectrum of the oxygenated solution was measured at  $-40$  °C (Figure 2). From this spectrum it was estimated that a single product formed in greater than 90% purity.

**Stoichiometry of Oxygenation of  $[\text{Co}(\mu\text{-OH})(\text{oxapyne})\text{Co}(\text{H}_2\text{O})](\text{ClO}_4)$ .** To a 0.05 M solution of  $[\text{Co}(\mu\text{-OH})(\text{oxapyne})\text{Co}(\text{H}_2\text{O})]\text{ClO}_4$  in dimethylformamide at 25 °C was added pure  $\text{O}_2$  via a syringe. The absorption of  $\text{O}_2$  was monitored by the disappearance of the electronic absorption band centered at 1015 nm ( $\epsilon = 12 \text{ M}^{-1} \text{cm}^{-1}$ ) displayed by the  $[\text{Co}(\mu\text{-OH})(\text{oxapyne})\text{Co}(\text{H}_2\text{O})]\text{ClO}_4$  complex. The band disappeared completely after 1 equiv of  $\text{O}_2$  was added.

**Isolation of the Oxygenation Product as a Solid.** The  $[\text{Co}(\mu\text{-OH})(\text{oxapyne})\text{Co}(\text{H}_2\text{O})]\text{ClO}_4$  complex (50 mg,  $55.3 \mu\text{mol}$ ) was dissolved in dry, deaerated  $\text{CH}_3\text{CN}$  (30 mL) to give a yellow solution. The volume of the solution was reduced to 3 mL under vacuum, and the solution was then cooled to  $-40$  °C. At this temperature dioxygen was introduced, producing a dark red solution. The solution was connected to a vacuum pump (0.5 mm), and, after pumping for a few minutes, the solution was removed from the bath. After  $\sim 15$  min, the solvent had been removed. The dark residue was slurried with diethyl ether at room temperature (10 mL), filtered, and washed with ether (5 mL) and pentane (5 mL) to afford the oxygenation product (45 mg, 80% pure by  $^1\text{H}$  NMR spectroscopy) as a dark brown solid. The remaining 20% of the material is an unidentified decomposition product. UV-vis ( $\text{CH}_3\text{CN}$ ,  $-40$  °C): 380 (14 780), 516 (shoulder, 2650).  $^1\text{H}$  NMR (500 MHz, 99.98% D  $\text{CD}_3\text{CN}$ ,  $-40$  °C):  $\delta$  8.60 (d, 1H,  $J = 4.0$  Hz), 8.56 (m, 2H), 8.08 (d, 1H,  $J = 8.5$  Hz), 8.03 (m, 3H), 7.85 (m, 3H), 7.58 (d, 1H,  $J = 7.4$  Hz), 7.43 (m, 7H), 7.19 (t, 2H,  $J = 6.8$  Hz), 5.32 (d, 1H,  $J = 17.9$  Hz), 4.59 (d, 1H,  $J = 13.6$  Hz), 4.51 (d, 1H,  $J = 17.9$  Hz), 4.35 (d, 1H,  $J = 17.6$  Hz), 4.21 (d, 1H,  $J = 15.3$  Hz), 4.13 (d, 1H,  $J = 17.7$  Hz), 4.07 (d, 1H,  $J = 15.3$  Hz), 4.00 (d, 1H,  $J = 13.8$  Hz), 3.49 (d, 1H,  $J = 15.5$  Hz), 3.16 (d, 1H,  $J = 15.1$  Hz), 2.66 (s, 3H),  $-2.42$  (s, 1H,  $\text{D}_2\text{O}$  exchangeable). IR ( $\text{cm}^{-1}$ ): 3376 (broad, OH), 1608, 1581, 1547, 1483, 1437, 1345, 1323, 1295, 1265, 1225, 1163, 1082 ( $\text{ClO}_4$ ), 1001, 983, 901, 875, 840, 763, 752, 721.

The reaction was carried out with  $^{18}\text{O}_2$  following the procedure described above, scaled down to 30 mg of the di-Co $^{2+}$  complex. A 2.5 mL amount of  $^{18}\text{O}_2$  was injected into the reaction mixture at low temperature. After removal of the solvent, the product was analyzed by  $^1\text{H}$  NMR spectroscopy and was found to be 82% pure.

The  $^{18}\text{O}_2$ -labeled complex gave an IR spectrum identical to the spectrum of unlabeled material.

**Oxygenation of  $[\text{Co}(\mu\text{-OH})(\text{oxapyne})\text{Co}(\text{H}_2\text{O})](\text{PF}_6)$ .** To a solution of  $\text{CoCl}_2 \cdot 6\text{H}_2\text{O}$  (100.2 mg, 0.41 mmol) in water (2 mL) was added a solution of  $\text{AgPF}_6$  (208 mg, 0.825 mmol) in water (3 mL). The

resulting white suspension was stirred for 15 min. It was filtered through Celite, and the filtrate was twice evaporated with  $\text{CH}_3\text{CN}$  to afford an orange residue. This residue was dissolved in a mixture of  $\text{CH}_3\text{CN}$  (1 mL) and water (80  $\mu\text{L}$ ) to give a pink solution. The preparation proceeded analogously to that of  $[\text{Co}(\mu\text{-OH})(\text{oxapyne})\text{Co}(\text{H}_2\text{O})](\text{ClO}_4)^{13}$  using this solution instead of a solution of  $\text{Co}(\text{ClO}_4)_2 \cdot 6\text{H}_2\text{O}$ . The  $[\text{Co}(\mu\text{-OH})(\text{oxapyne})\text{Co}(\text{H}_2\text{O})](\text{PF}_6)$  compound was precipitated as a yellow solid after diethyl ether (4 mL) was added and the suspension was stirred for 2 h. The yellow solid was filtered and was washed with an ether/ $\text{CH}_3\text{CN}$  mixture (1:1). The product (160 mg, 82%) was stored in a drybox and was used for oxygenation reactions.  $^{16}\text{O}$ - and  $^{18}\text{O}$ -containing oxygenation products were obtained following the procedure described above for the perchlorate analogue. They were characterized by  $^1\text{H}$  NMR and electronic spectroscopy. Attempts at obtaining FT-Raman spectra of these compounds were not successful, possibly because of their instability to the laser irradiation.

**$[\text{Co}(\mu,\eta^1:\eta^2\text{-O}_2)(\text{oxapyne})\text{Co}](\text{PF}_6)_2 \cdot \text{CH}_3\text{CN}$  (13). Method A.** The  $[\text{Co}(\mu\text{-OH})(\text{oxapyne})\text{Co}(\text{H}_2\text{O})]\text{ClO}_4$  complex (0.20 mmol, 181 mg) was dissolved in dry, deaerated methanol (100 mL) under  $\text{N}_2$  to give a light green solution after stirring for 2 h. After the solution was cooled to  $-78$  °C,  $\text{O}_2$  was introduced into the flask, and the color changed to red-brown in seconds. The solution became turbid after 30 min of stirring at  $-78$  °C. The mixture was allowed to warm slowly to  $-10$  °C to give a red-brown solution. A solution of  $\text{NH}_4\text{PF}_6$  (1.6 mmol, 0.26 g) in methanol (2 mL) was added to give a turbid solution. After the mixture was stirred for 1 h at room temperature, it was kept at  $-10$  °C for 15 h. The red-brown solid was collected and washed with methanol ( $2 \times 2 \text{ mL}$ ), ether ( $2 \times 2 \text{ mL}$ ), and pentane ( $2 \times 2 \text{ mL}$ ). After being dried under vacuum, 170 mg of red-brown solid was isolated. The product was recrystallized from a mixture of dry acetonitrile (5 mL) and methanol (10 mL) by diffusing with methanol for 2 days. Small brown crystals suitable for X-ray diffraction analysis were collected and were washed with methanol and ether. Yield: 70 mg (31%).  $\Lambda_{\text{M}} = 260 \text{ cm}^2 \Omega^{-1} \text{ mol}^{-1}$  ( $\text{CH}_3\text{CN}$ ). UV-vis (in  $\text{CH}_3\text{CN}$ ): 301 (20 130), 388 (14 252), 484 (sh, 2188). IR ( $\text{cm}^{-1}$ ): 2286 ( $\text{CH}_3\text{-CN}$ ), 1632, 1616, 1600, 1583, 1545, 1482, 1435, 1347, 1309, 1295, 1268, 1255, 1164, 1089, 1064, 1036, 904, 883, 829, 820 ( $\text{PF}_6^-$ ), 772, 762, 747, 718, 704, 671, 623. FT-Raman:  $839 \text{ cm}^{-1}$  ( $^{16}\text{O}$ – $^{16}\text{O}$  stretch).  $^1\text{H}$  NMR (400 MHz,  $\text{CD}_3\text{CN}$ ):  $\delta$  8.99 (d, 1H,  $J = 8.0$  Hz), 8.45 (d, 1H,  $J = 7.5$  Hz), 8.29 (d, 1H,  $J = 5.0$  Hz), 8.10 (s, 2H), 8.03 (t, 1H), 7.95 (s, 1H), 7.88 (t, 1H), 7.76 (t, 1H), 7.64 (d, 1H,  $J = 7.0$  Hz), 7.60 (t, 1H), 7.52–7.28 (m, 8H), 7.18 (s, 1H), 5.35 (d, 1H,  $J = 15.5$  Hz), 5.29 (d, 1H,  $J = 16.5$  Hz), 4.89 (d, 1H,  $J = 16.0$  Hz), 4.74 (d, 1H,  $J = 12.5$  Hz), 4.42 (d, 1H,  $J = 18.0$  Hz), 4.27 (d, 1H,  $J = 16.5$  Hz), 4.19 (m, 2H), 3.63 (d, 1H,  $J = 15.5$  Hz), 3.48 (d, 1H,  $J = 15.5$  Hz), 2.35 (s, 3H). ESI-MS:  $m/z$  400.5 [ $\text{M} - 2\text{PF}_6$ ] $^{2+}$ . Anal. Calcd for  $\text{C}_{39}\text{H}_{36}\text{Co}_2\text{F}_{12}\text{N}_{10}\text{O}_5\text{P}_2$ : C, 41.36; H, 3.20; N, 12.37. Found: C, 41.52; H, 3.37; N, 12.16.

The reaction was carried out with  $^{18}\text{O}_2$  following the procedure described above, where 10 mL of  $^{18}\text{O}_2$  was injected into the reaction mixture at low temperature. The product was analyzed by  $^1\text{H}$  NMR spectroscopy, mass spectrometry, and FT-Raman. ESI-MS:  $m/z$  402.6 [ $\text{M} - 2\text{PF}_6$ ] $^{2+}$ . FT-Raman:  $796 \text{ cm}^{-1}$  ( $^{18}\text{O}$ – $^{18}\text{O}$  stretch).

**Method B.** A solution of  $[\text{Co}(\mu\text{-OH})(\text{oxapyne})\text{Co}(\text{H}_2\text{O})]\text{ClO}_4$  complex (5 mg,  $5.53 \mu\text{mol}$ ) in dry  $\text{CH}_3\text{CN}$  (13 mL) was cooled to  $-40$  °C. Dioxygen was introduced, and the red solution was stirred for 5 min. A solution of  $\text{HClO}_4$  in  $\text{CH}_3\text{CN}$  (48  $\mu\text{L}$  of 0.115 M solution) was then added at  $-40$  °C. A yellow solution formed immediately. It was allowed to warm to room temperature over a period of 30 min. An orange solution formed. After the solvent was removed in vacuo, the product was found to be a mixture of  $[\text{Co}(\mu,\eta^1:\eta^2\text{-O}_2)(\text{oxapyne})\text{Co}]^{2+}$  (80%) and  $[\text{Co}(\mu\text{-OH})(\text{oxapyne})\text{Co}(\text{H}_2\text{O})]^{3+}$  (20%) by  $^1\text{H}$  NMR spectroscopy. ESI-MS:  $m/z$  400.6 [ $\text{M} - 2\text{ClO}_4$ ] $^{2+}$  (for the dioxygen complex).

The reaction was carried out with  $^{18}\text{O}_2$  following the procedure described above, where 3 mL of  $^{18}\text{O}_2$  was injected into the reaction



mixture at low temperature. The products were analyzed by NMR and mass spectrometry. ESI-MS:  $m/z$  402.6 [M - 2ClO<sub>4</sub>]<sup>2+</sup>.

**[Co( $\mu,\eta^1:\eta^2$ -O<sub>2</sub>)(oxapyme)Co](ClO<sub>4</sub>)<sub>2</sub>·2H<sub>2</sub>O** was prepared by a method similar to that for the PF<sub>6</sub><sup>-</sup> salt (method A), except that NH<sub>4</sub>-ClO<sub>4</sub> was used instead of NH<sub>4</sub>PF<sub>6</sub>. The product (120 mg) was recrystallized by slow vapor diffusion of ether into a solution of [Co( $\mu,\eta^1:\eta^2$ -O<sub>2</sub>)(oxapyme)Co](ClO<sub>4</sub>)<sub>2</sub> in a mixture of dry acetonitrile (7 mL) and methanol (15 mL). Needle-like dark brown crystals formed over a period of 3 days. They were filtered, washed with methanol (2 mL), ether (4 mL), and pentane (4 mL), and dried in a desiccator (50 mg, 27%). IR (cm<sup>-1</sup>): 1081 (ClO<sub>4</sub>). The product is pure by <sup>1</sup>H NMR spectroscopy. Anal. Calcd for C<sub>37</sub>H<sub>37</sub>Cl<sub>2</sub>Co<sub>2</sub>N<sub>9</sub>O<sub>15</sub>: C, 42.87; H, 3.60; N, 12.16. Found: C, 42.64; H, 3.44; N, 12.24.

**[Co( $\mu,\eta^1:\eta^1$ -O<sub>2</sub>)(oxapyme)Co(NO<sub>2</sub>)](PF<sub>6</sub>)<sub>2</sub>·2CH<sub>3</sub>CN (**14**), Method A.** To a solution of [Co( $\mu,\eta^1:\eta^2$ -O<sub>2</sub>)(oxapyme)Co](PF<sub>6</sub>)<sub>2</sub>·CH<sub>3</sub>CN (45 mg, 39  $\mu$ mol) in dry acetonitrile (50 mL) was added a solution of NaNO<sub>2</sub> (3.6 mg, 52  $\mu$ mol) in methanol (0.5 mL). The orange-red solution turned dark red immediately. It was stirred for 20 min and then was concentrated under vacuum to 2 mL. Acetone (2 mL) was added, followed by absolute ethanol (4 mL). The solution was diffused with ethanol vapor overnight at room temperature to afford dark red crystals. The crystals were filtered and washed with ethanol (2 mL), ether (4 mL), and pentane (4 mL). Dark red blades suitable for X-ray diffraction analysis were obtained (26 mg, 62%).  $\Lambda_M = 90$  cm<sup>2</sup>  $\Omega^{-1}$  mol<sup>-1</sup> (CH<sub>3</sub>CN). UV-vis (CH<sub>3</sub>CN): 412 (15 879), 497 (5360). FT-Raman: 866 cm<sup>-1</sup> (<sup>16</sup>O-<sup>16</sup>O stretch). <sup>1</sup>H NMR (400 MHz, CD<sub>3</sub>CN):  $\delta$  9.09 (d, 1H,  $J = 4.2$  Hz), 9.07 (d, 1H,  $J = 4.0$  Hz), 8.48 (d, 1H,  $J = 8.1$  Hz), 8.40 (d, 1H,  $J = 8.1$  Hz), 7.89 (t, 1H,  $J = 7.0$  Hz), 7.75 (t, 1H,  $J = 7.0$  Hz), 7.69 (d, 1H,  $J = 5.8$  Hz), 7.62-7.49 (m, 4H), 7.47 (t, 1H,  $J = 8.5$  Hz), 7.36 (d, 1H,  $J = 5.9$  Hz), 7.27-7.14 (m, 6H), 6.47 (t, 1H,  $J = 7.1$  Hz), 5.67 (d, 1H,  $J = 15.0$  Hz), 5.02 (d, 1H,  $J = 15.3$  Hz), 4.65 (d, 1H,  $J = 15.3$  Hz), 4.48 (d, 1H,  $J = 14.8$  Hz), 4.04 (d, 1H,  $J = 15.3$  Hz), 3.97 (d, 1H,  $J = 15.0$  Hz), 3.93 (d, 1H,  $J = 14.5$  Hz), 3.76 (d, 1H,  $J = 17.6$  Hz), 3.57 (d, 1H,  $J = 17.1$  Hz), 3.23 (d, 1H,  $J = 17.1$  Hz), 2.27 (s, 3H). ESI MS:  $m/z$  400.5 [M - NO<sub>2</sub> - PF<sub>6</sub>]<sup>2+</sup>, 815.1 [M - O<sub>2</sub> - PF<sub>6</sub>]<sup>+</sup>. Anal. Calcd for C<sub>41</sub>H<sub>39</sub>Co<sub>2</sub>F<sub>6</sub>N<sub>12</sub>O<sub>7</sub>P: C, 45.82; H, 3.66; N, 15.64. Found: C, 45.65; H, 3.48; N, 15.27.

The reaction was carried out with <sup>18</sup>O<sub>2</sub>-labeled [Co( $\mu,\eta^1:\eta^2$ -O<sub>2</sub>)(oxapyme)Co](PF<sub>6</sub>)<sub>2</sub>·CH<sub>3</sub>CN following the procedure described above. The products were analyzed by NMR, mass spectrometry, and FT-Raman. ESI-MS:  $m/z$  402.5 [M - NO<sub>2</sub> - PF<sub>6</sub>]<sup>2+</sup>, 815.0 [M - O<sub>2</sub> - PF<sub>6</sub>]<sup>+</sup>. FT-Raman: 825 cm<sup>-1</sup> (<sup>18</sup>O-<sup>18</sup>O stretch).

**Method B.** A solution of [Co( $\mu$ -OH)(oxapyme)Co(H<sub>2</sub>O)]PF<sub>6</sub> complex (1.6 mg, 1.68  $\mu$ mol) in CH<sub>3</sub>CN (4 mL) was cooled to -40 °C. Dioxxygen was introduced at this temperature. After the oxygenation reaction was complete, methanol (20  $\mu$ L) was added to the red solution. The color became somewhat lighter. A solution of NaNO<sub>2</sub> (0.915 mg,

13.3  $\mu$ mol) in methanol (92  $\mu$ L) was then added at -40 °C. The reaction mixture was allowed to warm to room temperature over a period of 30 min. A bright red solution formed. After the solvent was removed under vacuum, the product was identified by <sup>1</sup>H NMR spectroscopy as [Co( $\mu,\eta^1:\eta^1$ -O<sub>2</sub>)(oxapyme)Co(NO<sub>2</sub>)]<sup>+</sup> (90% pure).

**[Co( $\mu,\eta^1:\eta^1$ -O<sub>2</sub>)(oxapyme)Co(NO<sub>2</sub>)](ClO<sub>4</sub>)<sub>2</sub>·2.5H<sub>2</sub>O** was prepared analogously to [Co( $\mu,\eta^1:\eta^1$ -O<sub>2</sub>)(oxapyme)Co(NO<sub>2</sub>)](PF<sub>6</sub>)<sub>2</sub>·2CH<sub>3</sub>CN, starting with [Co( $\mu,\eta^1:\eta^2$ -O<sub>2</sub>)(oxapyme)Co](ClO<sub>4</sub>)<sub>2</sub>·2H<sub>2</sub>O. Upon recrystallization, the product was obtained as red crystals pure by <sup>1</sup>H NMR spectroscopy (53%). IR (cm<sup>-1</sup>): 3430, 1615, 1601, 1570, 1539, 1479, 1445, 1432, 1382, 1344, 1330, 1317, 1288, 1258, 1162, 1081 (ClO<sub>4</sub>), 1033, 962, 939, 915, 882, 863, 857, 819, 765, 772, 749, 742, 703, 671, 657, 623 cm<sup>-1</sup>. Anal. Calcd for C<sub>37</sub>H<sub>38</sub>Co<sub>2</sub>ClN<sub>10</sub>O<sub>13.5</sub>: C, 44.79; H, 3.86; N, 14.12. Found: C, 44.86; H, 3.74; N, 14.28.

**Reaction of [Co( $\mu,\eta^1:\eta^1$ -O<sub>2</sub>)(oxapyme)Co(NO<sub>2</sub>)](PF<sub>6</sub>)<sub>2</sub>·2CH<sub>3</sub>CN with HPF<sub>6</sub>.** To a deep red solution of [Co( $\mu,\eta^1:\eta^1$ -O<sub>2</sub>)(oxapyme)Co(NO<sub>2</sub>)](PF<sub>6</sub>)<sub>2</sub>·2CH<sub>3</sub>CN (2.9 mg, 2.7  $\mu$ mol) in deuterated acetonitrile (0.6 mL) was added a solution of HPF<sub>6</sub> (0.65 mg of 60% aqueous solution, 2.7  $\mu$ mol) in methanol (6.5  $\mu$ L). The red solution became lighter. The complex [Co( $\mu,\eta^1:\eta^2$ -O<sub>2</sub>)(oxapyme)Co](PF<sub>6</sub>)<sub>2</sub> is formed quantitatively by <sup>1</sup>H NMR spectroscopy.

**Crystallographic Structural Determination.** Crystallographic data are collected in Table 1. Data were collected using a Bruker P4 diffractometer equipped with a SMART 1000 CCD detector. In the case of **13**, systematic absences in the diffraction data uniquely determined the space group, and for **14**, the centrosymmetric alternative was selected initially on statistical considerations and confirmed by the stability of the refinement process. Despite the very small crystal size, high-resolution data were obtained by the use of long frame exposure times. Empirical corrections for absorption were applied using SADABS. The structures were solved by direct methods, and all non-hydrogen atoms were anisotropically refined. Hydrogen atoms were treated as idealized contributions. All computations and software are contained in the SHELXTL library of programs (G. Sheldrick, Bruker AXS, version 5.1, Madison, WI).

**Acknowledgment.** This work was supported by grants from the NSF and NIH. We thank Professor Michael Hopkins for use of his FT-Raman spectrometer.

**Supporting Information Available:** X-ray crystallographic file with listings of crystal data, atomic coordinates, thermal parameters, and bond distances and angles for [Co( $\mu,\eta^1:\eta^2$ -O<sub>2</sub>)(oxapyme)Co](PF<sub>6</sub>)<sub>2</sub>·CH<sub>3</sub>CN and [Co( $\mu,\eta^1:\eta^1$ -O<sub>2</sub>)(oxapyme)Co(NO<sub>2</sub>)](PF<sub>6</sub>)<sub>2</sub>·2CH<sub>3</sub>CN (CIF). This material is available free of charge via the Internet at <http://pubs.acs.org>.

JA012386Z